Advances in Science and Technology Research Journal

Advances in Science and Technology Research Journal 2024, 18(1), 167–183
https://doi.org/10.12913/22998624/177299
ISSN 2299-8624, License CC-BY 4.0

Received: 2023.08.28
Accepted: 2023.12.19
Published: 2024.01.15

Microstructure, Mechanical Properties, and Heat Distribution ANSYS Model of CP Copper and 316 Stainless Steel Torch Brazing

Auday Awad Abtan[1*], Mohammed S. Mohammed[1], Iqbal Alshalal[1]

[1] Training and Workshop Center, University of Technology-Iraq, Al-Wehda neighborhood, 19006, Baghdad, Iraq

* Corresponding author's e-mail: auday.a.abtan@uotechnolgy.edu.iq

ABSTRACT

Using torch brazing techniques, 316 stainless steel was brazed to CP copper using flux-coated low silver content filler with 20% Ag. The brazing torch utilized a fuel mixture of propane gas with oxygen to produce the required heating amount due to the possibility of economic interest in employing low-silver-content filler. The brazing filler's braze ability with SUS304 and copper was scrutinized and deeply analyzed. A ferrite barrier layer was made on the stainless-steel side, and an excellent brazed joint was produced. Metallurgical studies using an optical microscope and a scanning electron microscope (SEM) confirmed the production of a ferrite layer. This layer's advantages were carefully examined with metallurgical testing, electron diffraction scanning (EDS), EDS mapping, and EDS line analyses, including preventing copper intergranular penetration into the stainless-steel grain boundary. The mechanical properties of the brazed joint and its usability were assessed through Vickers microhardness and tensile tests on the brazing seam and both base metals. The results of the brazing process showed that using flux-coated low-silver brazing techniques produced strong joints with satisfactory mechanical properties. These techniques are a cost-effective alternative to high-priced brazing fillers with high silver content. Geometrical models simulated the heat distribution using ANSYS and SOLIDWORKS software to analyze penetration depth, joint quality, surface cracks, and the relation between molten filler density variation and the wetting process.

Keywords: brazing, dissimilar joint, copper, stainless steel, ANSYS.

INTRODUCTION

Due to their electrical and corrosion resistance properties, copper and stainless-steel dissimilar joints are widely used in various industries. However, joining copper with stainless steel is challenging in modern manufacturing. The lack of unity between stainless steel and copper in terms of their mechanical, thermal, and chemical properties complicates this joining. It is challenging to achieve copper-to-stainless steel dissimilar jointing without any defect using conventional fusion welding methods like gas tungsten arc welding, submerged arc welding, shielded metal arc welding, and gas metal arc welding due to the difficulties in controlling the formation of undesirable phases and cracks formation in welding zone [1]. Fusion arc welding technology is a significant copper and stainless-steel welding technology due to its flexibility and low cost. However, in arc welding technology, the base metal representing one of the welding arc electrodes immediately absorbs welding arc heat and melts. Excessive fusion of the welding zone results in total dilution and circulation between Fe base metal and Cu, increasing Cu content inside the welding interface. At the same time, due to the base metal's high thermal expansion, stresses would be generated and then concentrated at the welding interface when directly heated by the focused energy of the welding arc. Therefore, when tensile stress is applied, a crack from copper penetrating would occur. The copper penetrating phenomenon has essential acts in austenitic stainless-steel embrittlement. This crack type can be found in

grain boundaries between the stainless-steel interface and the joining fusion zone (FZ) [2, 3]. According to earlier research, molten liquid copper diminished stainless-steel strength by up to 35% and decreased elongation by up to 73% [4]. Brazing joining was often used in dissimilar joint fabrication in the past years. However, the problem with these joints' quality was required to vacuum technology during this process, which often influenced determining the joint's quality [5]. Cu to stainless steel brazed joints is widely used in cooling and heating systems, refrigerators, and food-freezing equipment [6]. The selection of filler or an electrode material compatible with parent metals is one of the significant challenges facing this joining. Dissimilar metal joining is considered a complicated bonding technology compared to similar metal joining, as investigated by Devendranath et al., due to thermal and chemical properties alterations. Significant problems with these joints were the solubility problems resulting from the chemical composition difference between metals to be joined [7]. A mismatch in the value of the thermal expansion coefficient between two materials to be jointed also resulted in major joint failure as sequenced by thermal fatigue. Melting one of the base materials before the other due to the difference in melting point and thermal conductivity could cause a lack of fusion defects. In these situations, the preheating process should be used with higher thermal conductivity material before welding, as Sajjad et al. [8] reported when investigating AISI 304 GTAW with copper. AISI 304 is one of the most used types of stainless steel. Still, its low dissipation of heat when serviced at high-temperature conditions causes the creation of undesirable phases, which influence its mechanical properties reduction. When joining copper to stainless steel, stainless steel's inadequate heat dissipation can be improved with copper, which has good thermal conductivity. These joints, in turn, will prevent undesirable phase formation like chromium carbide precipitation and sigma phase. Filler metal selection is compatible with both metals and is critical in joining stainless steel and copper. Improper filler metal selection produces defects like porosity, hot cracks, shrinkage, fusion lack, and decreased tensile strength, as detected by Sajjad et al. [8]. Joining dissimilar metals like copper with 304 stainless steel includes many applications in food processing and vessel industries, reported by Durgutlu et al. [9], to employ excellent corrosion resistance and high strength of stainless steel with copper's significant electrical properties and high thermal conductivity [9]. Copper and AISI 304 joints are widely used in the heat transfer devices industry. It has been reported in Magnabosco et al. research that such joints have critical and essential applications [10]. Velu et al. have provided results showing that these weldments' performance cannot be predicted and requires further investigation to understand their properties fully. Joining stainless steel with copper requires a proper selection of fillers and electrodes. Previous research [11] shows that nickel-based fillers and electrodes offer better results than bronze fillers and electrodes. Bronze fillers can cause hot cracks and porosity defects, making them less desirable. However, nickel-based fillers and electrodes are recommended due to their improved mechanical properties and enhanced solubility of copper and iron. The research also suggests that controlling and limiting the amount of molten copper from brazing filler dissolved in steel is essential to achieve joints without defects. Regarding stainless steel to copper pipe brazing, Ag-based brazing filler is traditionally used. The best results have been achieved using BAg8 eutectic Ag-based filler. Although it has good brazed ability, unfortunately, this filler's high Ag content makes it costly. Fillers with low-silver content could be an economical option when selecting less expensive brazing filler metal; however, the issue with these fillers, as shown in Figure 1, requires a higher liquid temperature than BAg8 eutectic filler. High brazing temperatures had terrible effects on joining because they suppressed brazing wetting between filler and base metal. Also, these fillers had high Cu content. Decreasing Ag content in filler metal would increase fluidity due to increased melting temperature with increasing Cu range. Therefore, this investigation investigates and discusses stainless steel to copper brazed with flux-coated low silver filler metal and the braze ability of flux-coated low silver filler torch brazing techniques [12]. Stainless steel to copper torch brazing joining offered significant advantages due to the excellent mobility of the brazing torch and the ability to reach critical join complicated design; also, the torch brazing had the benefit of locally heating the brazed joint without exposed metal out from entering to undesired heating [13].

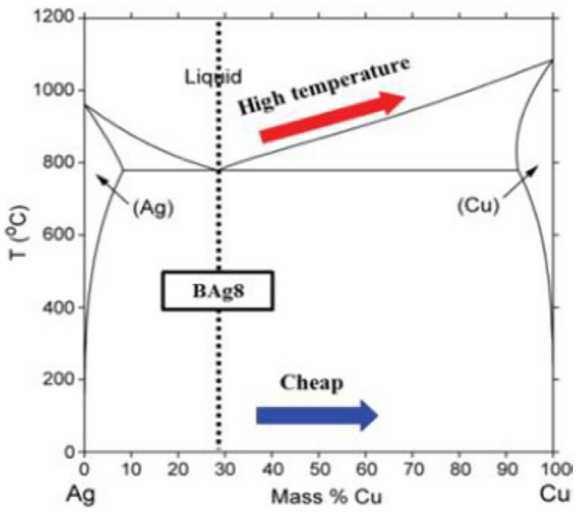

Fig. 1. Ag/Cu binary phase diagram

High-temperature localized brazing techniques, such as torch brazing, are frequently used in the aerospace, chemical, and power generation industries to join parts that cannot fit inside a furnace, like compressor impellers or turbine parts. During service, these parts experience various loading conditions, including thermal, mechanical, and corrosive. Therefore, stainless steel is commonly used to manufacture these parts due to its good combination of mechanical strength and corrosion resistance [14, 15].

EXPERIMENTAL MATERIALS AND PROCEDURE

316 austenitic stainless steel has an 18 mm inner diameter and 20 mm outer diameter, and commercially pure copper has a 20 mm inner diameter and 22 mm outer diameter. Brazed specimens were used in this investigation. A solid work schematic diagram of a torch brazing tube joint used in this investigation is illustrated in Figure 2. Low-silver-content flux-coated torch brazing filler wire was used with 20% silver brazing filler. Base metal tubes and flux-coated low silver brazing commercial filler chemical compositions with filler melting temperatures are listed in Tables (1-3). A mixture of propane and oxygen was used as brazing fuel to generate the required brazing temperatures between 780 °C and 810 °C to melt the low silver contain filler. The flux-coated brazing rods already have the flux in the rod, a product that is easier to use. It is essential to consider the type of finish required. Both tubes were cleaned with oil removal, acetone, and water to remove any chemical trace of oil removal and well drying just before the torch brazing. Stainless steel tube inserts inside the copper tube with 0.1 to 0.14 mm tolerances between the two surfaces and about 70 mm deep.

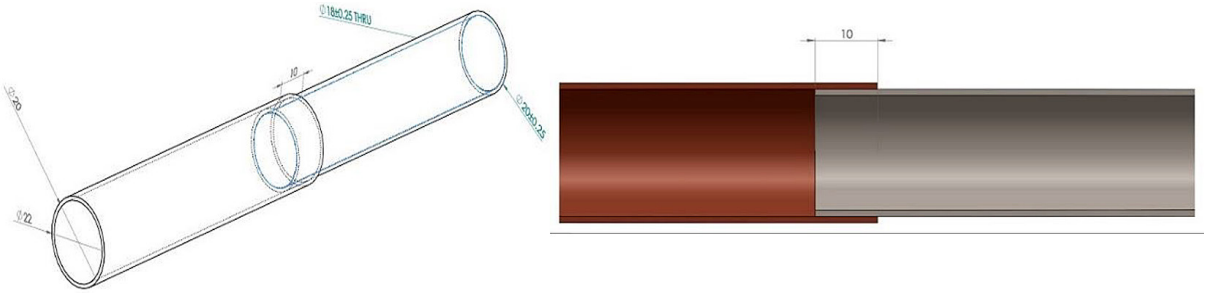

Fig. 2. Schematic of geometry and configuration

Table 1. filler metal chemical composition and melting temp

Silver	Copper	Zinc	Silicon	Melting Temp.	Solidus Temp.
20	44	36	0.15	810	690

Table 2. AISI 316 stainless steel base metal chemical composition

C	Si	Mn	P	S	Ni	Cr	Mo	N	Fe
0.08	0.60	1.7	0.04	0.028	12	17	2.4	0.08	Balance

Table 3. Copper base metal chemical composition

Cu	P	S	Ni	Fe
99.99	0.001	0.002	0.002	0.002

After that, about five samples were torch brazed and long tail cuts to test the microstructure, filler metal penetration, microhardness, SEM, EDS, and tensile tests for testing and estimating the joint microstructure and mechanical properties.

Microstructure, SEM, and EDS test

After brazing, a 30 mm long specimen was cut for metallographic observation, including the brazed joint at the center of the prepared sample. Then, a specimen is polished with grinding papers starting from 150 to 2000 grit size, and fine polishing is done on the specimen surface with the diamond paste by a polishing machine. For microstructure observation, specimens etched in the following reagents: HCL (15 mL) + HNO_3 (5 mL) for 316 stainless steel and (10 grams $CuSO_4$ + HCL 50 mL + H_2O 50 mL) copper base metal and joining zone. Then, the etched sample was observed with an optical microscope (OM) (Radical 2000 x Metal Alloy Grain Testing Metallurgical Top Light Microscope w XY Stage) for microstructural analysis of various joint zones. Scanning electron microscope (SEM EM-30 Series) with energy dispersive spectrometers (EDS) imploded to evaluate elements distribution inside the brazed joint and diffusion zone and its transformation between joining and diffusion zones from both sides.

Vickers microhardness tests

Vickers microhardness tests of the Cu to SUS316 tubes were done over the entire cross-section of all five zones (stainless steel base metal zone, stainless steel diffusion zone, brazed joint area, copper diffusion zone, and finally, copper base metal zone) to record the hardness profile. The testing done by (Micro Hardness Tester – Turret Control, Manual Software (900-391C)) device, testing applied load was 200 grams for the CP copper side and 500 grams employed when testing the remaining four zones. Testing dwell time was 10 seconds, and microhardness was recorded every 0.25 mm.

Tensile test

Rectangular transverse tensile test samples were prepared from the brazing tubes using a wire-cut machine to test the tensile shear strength and estimate the joint mechanical properties between CP copper and AISI316 stainless steel. Tensile strength was measured using a 200 kN (20000 kgf) Universal Tensile Testing Machine, Model TB20T device produced by China with cross-head 0.5 mm/min moving speed. Three tensile test samples were tested to ensure the reliability of the results. The tensile testing is performed after extracting tensile specimens from welded samples along the transverse direction of the pipe joints as per the standard dimensions mentioned in Section IX of the American Society of Mechanical Engineers (ASME) standards, as shown in Figure 3.

Thermal analysis with ANSYS models

Thermal distribution along the brazed joint was investigated, and the temperatures along the interface between stainless steel and copper were tested and analyzed with ANSYS thermal models. The heat distribution along the joining interface is essential to determine and predict the joint depth. How far the molten filler can penetrate inside the joining area, this parameter is critical in determining the joint strength and the part usability.

RESULTS AND DISCUSSION

Brazing microstructures analyzing

The explained microstructure showed exemplary metallurgical bonding cross-sections between the low silver brazing filler and both base

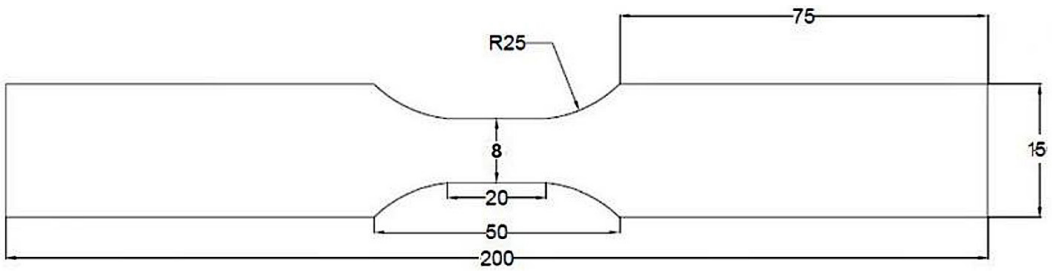

Fig. 3. Tensile test sample scheme

metals from both sides. Flux-coated silver brazing 20% silver revelation an excellent fluidity based on its good fillet pentation even when surface temperature drops and increases the molten filler density. Conversely, the fluidity of flux small silver content brazing plaster is less than traditional high-silver fillers such as BAg8, according to earlier research [16]. Cu base metal dissolution occurred moderately during brazing when brazed with fillers without flux. Still, when flux-coated low-silver filler was used, Cu metal dissolution became extensive compared with high silver fillers due to the relatively high copper percentage and high liquid temperature of low silver filler. A significant problem when joining copper to steel alloys is the intergranular liquid metal penetration of molten copper into the steel grain boundary, as shown in Figure 4, which causes cracks in base metal. Tensile stress is expected to develop at the brazed joint zone between copper from molten filler and steel when brazing heat is applied; this heat would agitate open micro-cracks with critical bulk close to the brazing solid/liquid edge from the steel side due to metallic embrittlement [17]. This process is prejudicial to the durability of joining structures, preventing Cu penetration usually achieved by controlling the process parameters when possible or by the metallurgical approach, which is more effective. The metallurgical system is based on ferrite having admirable intergranular infiltration struggle against smelted copper perception compared with austenite. Harmful copper intergranular penetration can be inhibited by producing a thin ferrite sheet as an obstruction. The adequate technique adds elements to copper, working as a ferrite stabilizer and promoting ferrite formation in the brazed joint interface. Zn, Si, and other elements could be practical ferrite stabilization elements. These elements have significant diffusion coefficients in steel and are beneficial for controlling interface interfacial reactions.

The brazed joint microstructure in Figure 5 demonstrates the formation of this barrier layer between brazing filler and stainless steel. Figure 4 A, B, C, and D reveal continuous but un-uniformed ferrite layers of α-iron and zinc. The creation of this layer in flux-coated low silver brazing filler will depend essentially on the diffusion mechanism of Zn in Fe. The brazing heat amount will govern the formation of the ferrite barrier layer, and its composition can be predicated on the Fe-Zn binary diagram shown in Figure 6. This phase diagram shows that magnetic transition happens in α-Fe below 770 °C temperatures. Fe-Zn phase diagram, also illustrated at 700 and 750 °C on magnetic transition line, Zn percentage must be between 3.3 and 11.5 for transition to magnetic characteristics. Based on their research, the authors suggest that the thickness and concentration of the ferrite layer could have led to the formation of two phases of ferromagnetic and

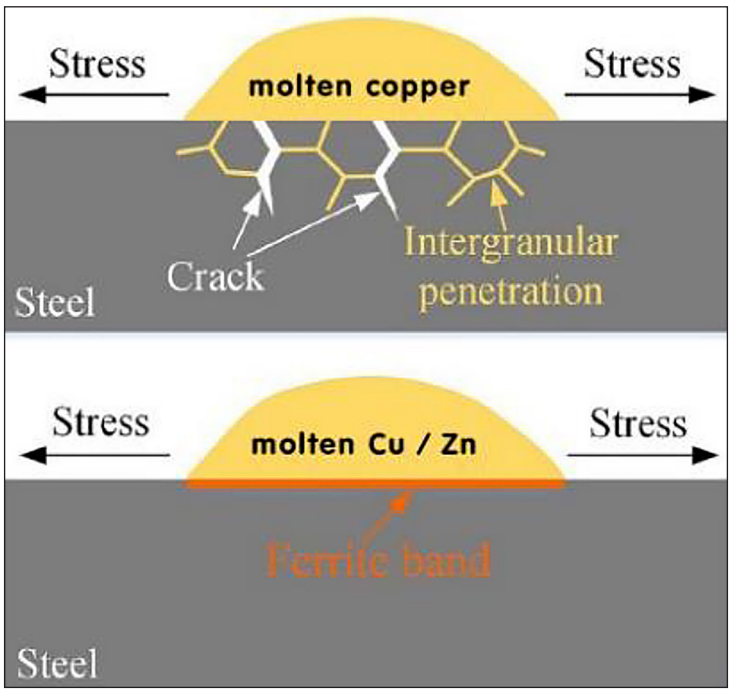

Fig. 4. Mechanism of ferrite barrier hindering intergranular liquid copper penetration into steel

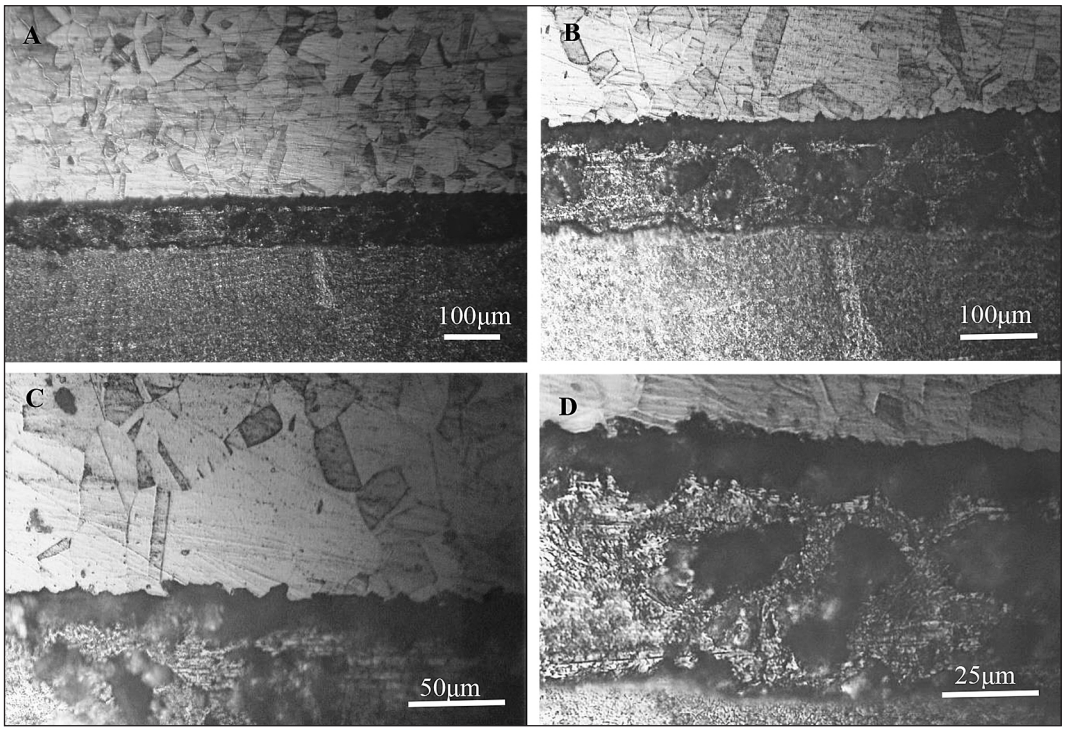

Fig. 5. Ferrite barrier in stainless steel joints side. (A) magnification of 10X. (B) 20X. (C) 40X. (D) 80X

paramagnetic -Fe, which may have undergone magnetic evolution. [18].

The Ferroscope was used in this investigation to measure the ferrite percentage in the barrier layer depending on the magnetic transition and detect the ferrite formation. Fe-Zn phase diagram illustrated that the γ-Fe When the temperature is between 912 and 1394 °C, the phase is steady and stable below 780 °C. [19]. No γ-Fe phase is expected to be found in the barrier layer in this investigation due to the brazing filler molten temperature at 810 °C. The liquid Zn solidified upon cooling the Fe/Zn phases, producing inhomogeneous microstructures of two phases. This solidification process caused segregation in the solidified liquid, resulting in significant variation in the composition of the brazing seam [20]. At 900, 850, and 800 °C temperatures, the solidified Fe/Zn liquid forms α-Fe and three types of microstructures. In contrast, at temperatures of 750 and 700 °C, the molten metal solidifies into two phases, Γ and α-Fe. As the amount of Zn in the molten brazing metal increases, the inter-diffusion coefficients between the two phases also rise. The current inter-diffusion coefficients cover the complete compositions of the -Fe and single-phase area [21]. From the above, we can conclude that forming a ferrite layer is essential in inhibiting molten Cu intergranular penetration inside the steel. Zn diffusion behavior is critical during brazing seam formation between steel and molten filler rich in Zn and copper. Chemical potential is the Zn diffusion driving force since the assistance of other elements in Zn distribution and liquid Cu penetration is very small; the contribution of these components will be abandoned and will not be investigated in this experiment's discussion about Zn diffusion behavior. Steel dissolves into a liquid phase when solid stainless steel is wetted with Zn from molten brazing filler. Alloying elements like Fe and Cr may diffuse from stainless steel toward liquid filler, resulting in Zn chemical potential alterations inside liquid phase approach solid/liquid interface. When the mole fractions of Fe and Cr rise, the chemical potential of the Zn element falls. Dissolving stainless steel would raise liquid phase Fe and Cr concentrations close to the solid/liquid boundary and lower Zn's chemical potential. To create an unformed thickness barrier layer between the copper and base metal, Zn continually collects inside the molten filler approach brazing seam diffusion line with stainless steel and spreads in the direction that was discovered to be from liquid to solid/liquid zone. This demonstrates that Zn diffusion is accomplished through diffusion and Zn mass transfer.

Zn must diffuse from molten filler into stainless steel to promote ferrite layer formation between the brazing interface and stainless steel. When Zn diffused in the direction of stainless

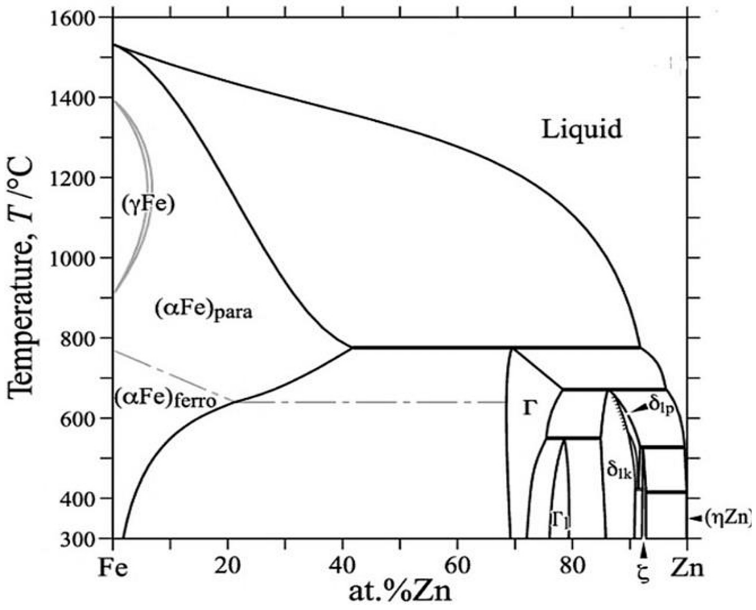

Fig. 6. Fe / Zn phase diagram

steel, Cr and Fe are presupposed to be a constant ratio. Zn chemical potential increased when Zn increased due to the increase in diffusion rate when the temperature rises until a specific temperature. The chemical potential of Zn in stainless steel will be lower than this element's chemical potential inside molten filler when the Zn mole fraction is identical for both. The Zn molar fraction of stainless steel in the brazing diffusion line is lower than molten filler during the initial interfacial response stage, enhancing the difference in Zn chemical potential between the two materials. Additionally, as the temperature increased, the chemical potential of zinc dropped significantly. The slight reduction in chemical potential caused by increasing temperature was insufficient to inverse the direction of Zn diffusion. Therefore, Zn behavior piling up inside molten filler in a brazing diffusion line with stainless steel induces further Zn diffusion because of considerable differences in chemical potential [22]. The surface energies at the boundary are crucial when estimating the depth of filler penetration. Per the laws of thermodynamics, a decrease in surface energy drives the nucleation and growth of new phases. This decrease occurs due to a significant misalignment in grain boundary energy (γgb) between solid-liquid interfaces, resulting in a lower system energy (γsl). In essence, 2(γsl) < (γgb). To comprehend the intergranular penetration mechanism, we must understand how ferrite behaves. When the system temperature is below 930 K, ferrite exhibits lower Gibbs free energy than austenite [23]. Temperature increases with Zn content increasing inside the system until Zn content reaches a specific amount; then, ferrite will have Gibbs energy less than austenite in wholly system temperatures. Therefore, ferrites can form inside the barrier layer according to these experimental situations. Studies on the wetting theory of grain boundaries and related experiments have indicated that ferrite exhibits strong resistance to liquid copper intergranular penetration. As a result, it is possible that conventional wetting theory does not have a significant impact on micro-intergranular penetration. Current investigation experimental conditions compared with traditional wetting theory indicate wetting mechanisms could be connected to Zn diffusion and accumulation in the brazing diffusion line because the ferrite band layer contains a high Zn percentage due to reduction expected in both Zn and Cu scheduled to reduce in steel's solidus and liquids considerably.

Brazing SEM and EDS line map analysis

Figure 7 displays the SEM images of flux-coated brazed joints with low silver filling. The SEM image shows the copper side on the right and the stainless-steel side on the left. A good surface without micro cracks but with some slag inclusion can be observed at the start of brazing, as shown in Figures (7) (A) and (B); good intersecting zones between the brazed joint and both sides can also be seen. In Figure 7 (C), when moving deeply inside the end of the joint, a gray-black

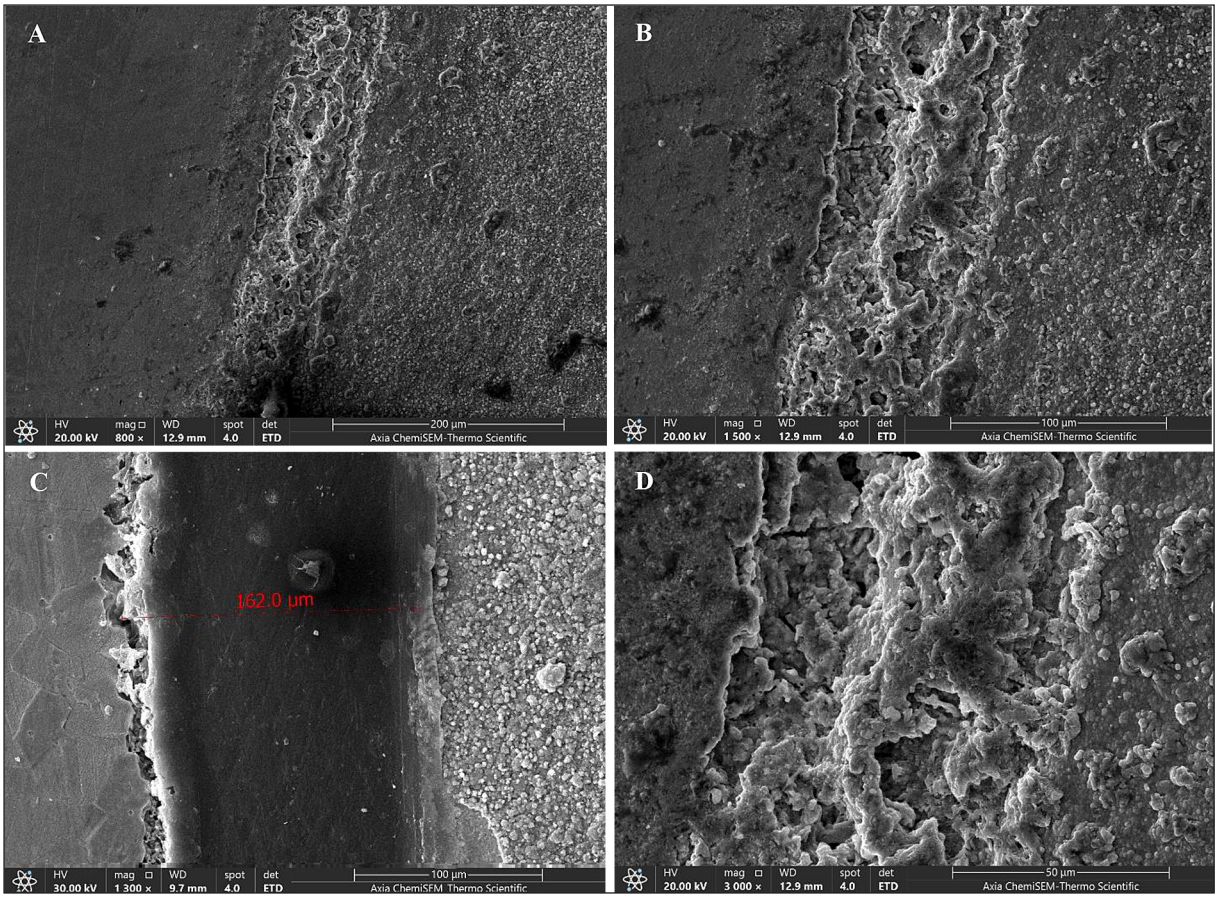

Fig. 7. SEM images of (A) and (B) Brazed joint with two base metals sides at the starting of the joint, (C) SEM image at the joint end with a micro crack along the stainless-steel side, (D) SEM image of the brazing solidified filler metal

crack starting in the ferrite barrier layer is observed with a 5.4 to 20 µm size and irregular width along the intersecting zones between the brazed joint and stainless-steel side. This study's authors explain this due to the drop in brazing temperature when the distance increases from the heat source at the joint starting; also, the high thermal expansion of stainless steel plays an essential role in this process. Figure 7 (D) SEM image demonstrates the brazed joint metal, rough gray-black phase of Cu-based solid solution observed in this zone.

The energy spectrum chemical compositions of the phases in Figure 7 (A) show scanning outcomes from the energy spectrum of the metal. Consistent with the Cu/Fe and Fe/Zn phase pictures, when the temperature reaches 850 °C, Zn and Cu effectively dissolve in Fe when Zn solid solubility is higher than Cu [23]. However, brazing filler with Ag content has serious dissolved problems in α-Fe [24]. EDS results in Figure 8 (B) show the transition brazing line between brazing filler solidified metals and stainless-steel side; the results reveal the high concentration of Zn and Fe with low Ag percentage, which gives strong evidence about the ferrite layer formation. EDS results of the brazed surface micro-crack at the brazed joint end show strong proof of the ferrite barrier layer; Table 4 lists chemical analysis of the brazed seam and Table 5 lists the transition line between stainless steel base metal and brazing metal chemical composition. Line scanning results in Figure 9 show Cu, Zn, and Ag diffusion degrees in the brazed flux-coated low silver filler joint metal. At the same time, energy spectrum scanning results show that the scanning area where the step-like shape is where the copper component diffusion will be greater than the silver and create the solid copper-based solution. [25]. While concave–convex energy spectrum scanning area is at an exact Figure of the Ag/Cu eutectic region, silver diffusion is higher than copper in this region, and solid solutions with silver-based will be formed [26]. The periodic table shows that Ag and Zn have distinctive periods, but Zn and Cu have a standard period. The atomic diameter difference between copper and zinc is

smaller than the variance between silver and zinc atomic diameter; at the same time, Zn solid solubility in Cu is more excellent than Zn in Ag [27]. Consequently, when the temperature decreased, Zn and Cu solid solution had high melting point crystallization [28]. Remaining Cu and Zn atoms in the liquid phase diminish as solidification progresses. A silver-based solid solution was created when Cu and Zn dissolved in Ag at a low melting point due to the temperature drop. The residual liquid will form a (Cu + Ag) eutectic structure as the system temperature steadily drops to the eutectic point [29]. Scanning results from the energy spectrum of flux coating low silver base filler brazing seam are shown in Figure 11; copper and silver elements distribution observed insides

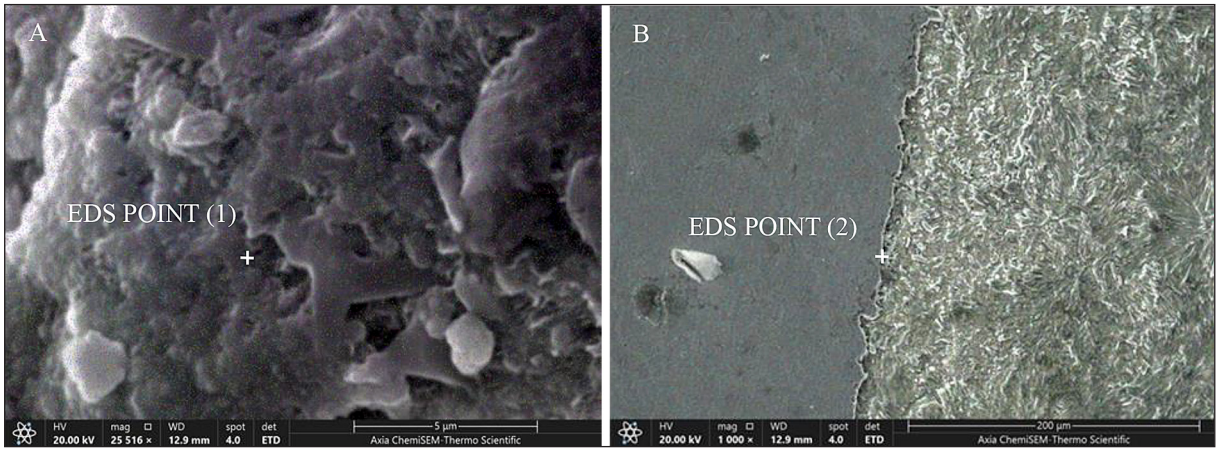

Fig. 8. EDS analyses the location of (A) brazing solidified metal and (B) brazing transition line between the braze metal and stainless-steel side

Table 4. EDS chemical analysis of brazing solidified metal (point 1)

Element	C	O	Cl	Cu	Zn	Rb	Nb	Ag
Weight %	1.0	8.4	1.8	32.4	34.9	0.5	1.9	19.2
Weight % Error	----	0.2	0.1	0.4	0.5	0.1	0.2	0.3

Table 5. EDS chemical analysis of brazing transition line (point 2)

Element	C	O	Fe	Cr	Ni	Cu	Zn	Ag
Weight %	7.8	20.3	13.0	11.9	7.9	1.5	20.3	17.4
Weight % Error	0.4	0.4	0.6	0.2	0.3	0.4	0.6	0.4

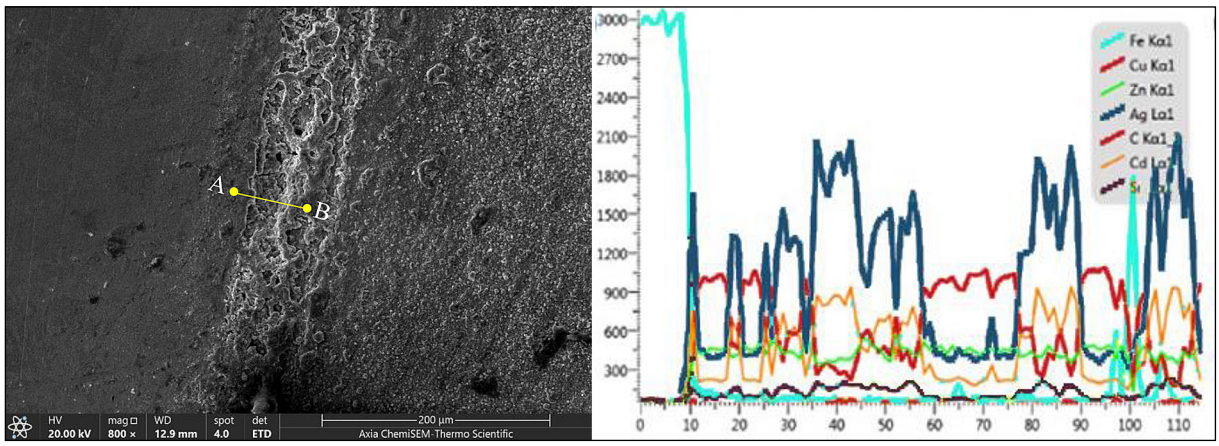

Fig. 9. Line map EDS scanning results between points A and B crossing the brazed joint

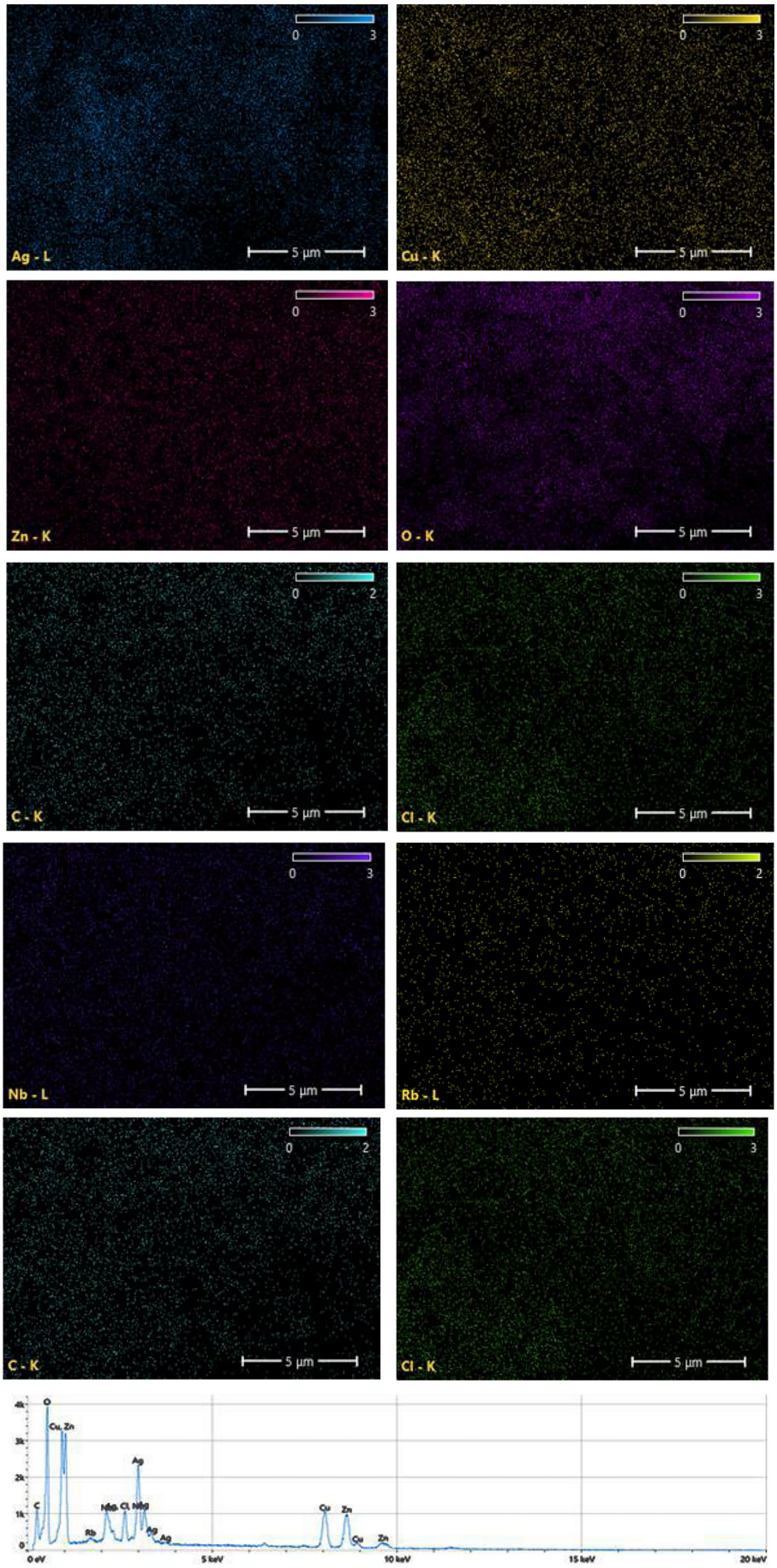

Fig. 10. Elements distribution map EDS scanning results of solidified brazed joint

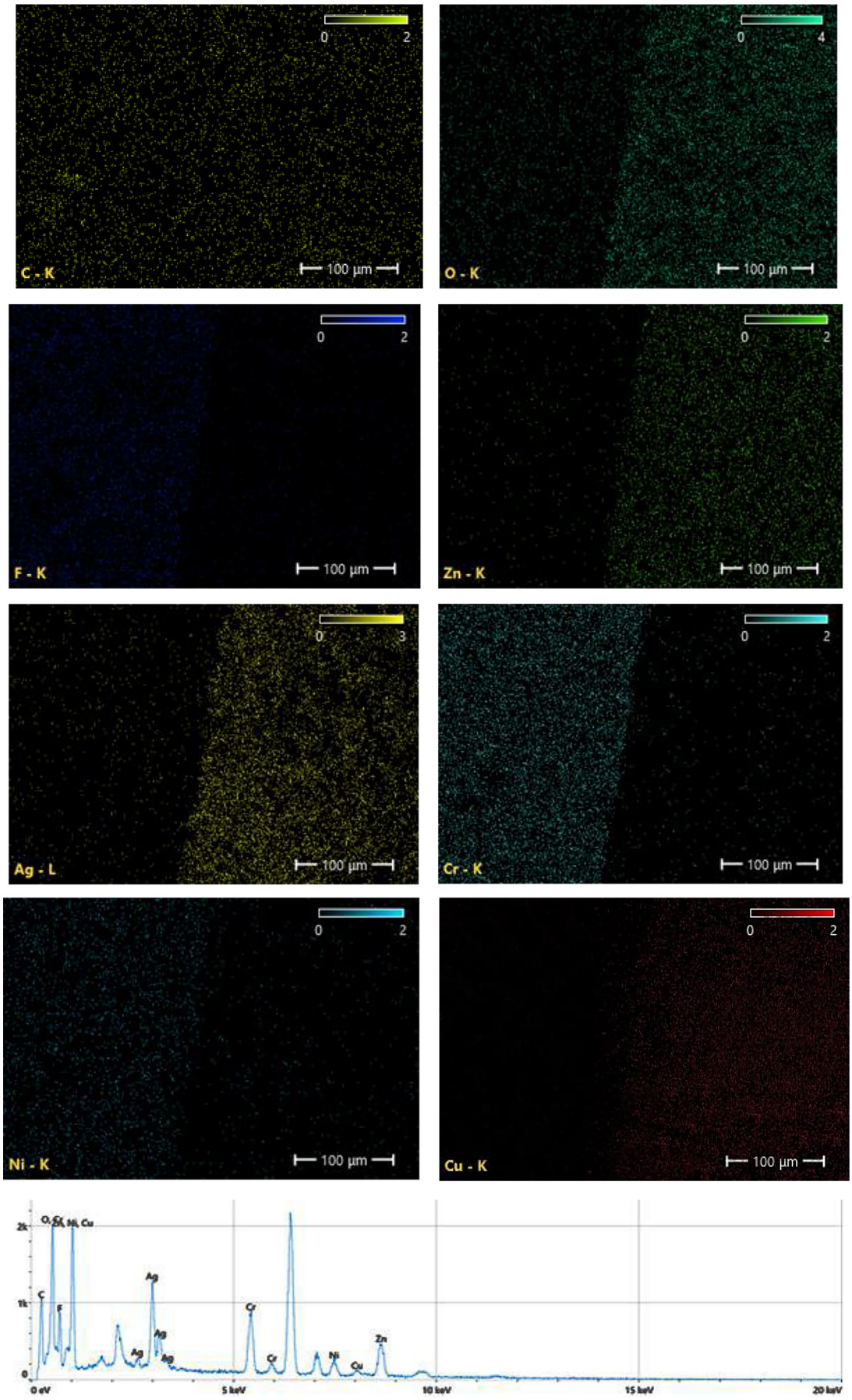

Fig. 11. Elements distribution map EDS scanning results of intersection brazing line between brazing metal and stainless steel side

can be realized that Cu interface in the brazed joint using flux coating low silver filler is distributed uniformly inside the solidified joint metal. In contrast, Ag is closely distributed in clusters around Cu and connected. Without segregation, a uniformly distributed Zn model can be seen in the (Cu + Ag) eutectic phase, silver- and copper-based solid solutions [30]. The joint intersection elements distribution EDS result between the solidified brazing seam and stainless steel in Figure 11 illustrates the high concentration of Zn in the brazed joint without passing to the stainless-steel side. Also, the results realized the Cu high concentration inside the joint without any trace or affected presence on the stainless-steel side. These results proved the ferrite barrier's successful work in preventing Cu's intergranular penetration into the Fe grain boundaries. The EDS map images in Figure 10 show no Ni and Cr elements distribution inside the brazed metal, while there is a good distribution of C in the joining seam. Brazing techniques depend on wetting phenomena between molten filler and base metal. Chromium oxide surface film-reducing techniques based on carbon achieve wetting in stainless steel with high carbon. However, this effect may not be practical in joining seams due to the absence of Cr, and in sequence, there is no chromium oxide film to reduce. The EDS map images illustrated high Ni and Cr element concentrations in the 316 stainless steel intersection with the brazing seam in Figure 11. The Mn presence in base metal in the 316 base metal side and intersection line helps the wetting process [31]. Further, Ni high content in the 316 base metal also participates in better wetting with the braze metal.

Mechanical properties of brazed joint

The brazed joint microhardness was measured using the HV-1000 microhardness tester with a 200 gf testing load and 10 s dwell time. The represented results in Figure 11 are for the s. The Microhardness curve in Figure 12 shows that brazed joints' hardness values are significantly higher than the base metals. The maximum microhardness is 151 HV at the center of the flux-coated low silver filler brazed joint metal, and the minimum is 100 at the intersection between brazing metal and stainless steel due to the softness effects of the ferrite layer in this zone. These results reflected the formation of the high hardness phases of Cu-Zn inside the brazing metal joint; these phases will reduce the joint toughness and affect the fracture location point during the tensile test. Also, it will reduce the shear results of the brazed joint. Universal Tensile Testing Machine (200 kN), Model TB20T, used in testing brazed joint tensile and shear strength. During the shear test, the specimen that brazed with a 10 mm overlapping length finally failed at the overlapping joint. The brazed joint average tensile strength is 152 MPa, and the shear strength is 102 MPa. Results show that the mechanical properties of flux-coated low silver s obviously have good brazed joints. The authors explain these results due to the Cu-based solid solution's small size inside the brazed joint metal. This small size is equivalent to grain refinement effects inside the joining structure. Also, these results indicate minimal or no formation in some cases of the eutectic (Cu + Ag) phase at the brazed joint [32]. This study investigated the differences between flux-coated low silver filler properties and silver-based solid

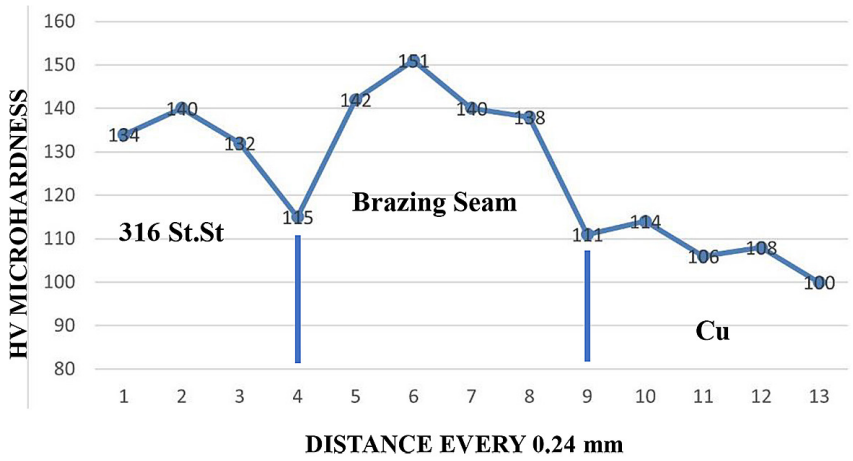

Fig. 12. Vickers microhardness profile of two base metals and brazing seam

solutions fillers. Still, this filler consists of more considerable microstructure alterations incorporated with small needle-like eutectic silver copper than traditional Ag filler. Compared with both parent metals, the microhardness of the brazed joint is considerably increasing, reaching 151 HV; this number is higher than both base metal microhardness. Its tensile and shear strength are generally lower than other Ag fillers's.

Brazed joint mathematical and ANSYS heat distribution models

The torch brazing process has many complexities associated with its technology; making direct observation is very difficult for the present visualization technology. Fortunately, mathematical and numerical simulation provides a valuable way to qualitatively reduce the experimental details and undiscovered physical mechanisms in the torch brazing process. During the torch brazing, parent metals' temperature rapidly changes. Defining parent metals' thermal properties in different brazing temperatures is necessary to achieve exact heat distribution simulation results. Metals' thermal physical properties, such as density, did not dramatically alter with temperature variation during brazing and, according to that, can be treated as constant values depending on the base metal type. In this paper, ANSYS software calculates parent metals' thermal properties in different temperatures and is checked by a literature search for more accurate results [1, 16, 17]. The thermos physical properties of both stainless steel and copper were established in simulation by setting up the convection and heat flow for both metals as boundary conditions for simulation results. The assembly of the geometrical model involves two tubes, each with a 1 mm wall thickness and outer diameters of 20 mm for stainless steel and 22 mm for copper. This was achieved using Solid Work software and then imported into ANSYS for simulation purposes, as depicted in Figure 13. The geometrical element mesh in Figure 14 was generated using ANSYS MESH software, resulting in 6128 elements and 40938 nodes, with a default size of 0.005.

Simulation results accuracy is evaluated by comparing this study's simulated temperature field with brazed joint cross-section metallography results. Figure 15 shows temperature distribution field of the brazed joint and brazing overlap. The maximum brazing expected temperature is 850 °C as can be seen from Figure 15, which is above the melting point of the brazing filler alloy; this temperature simulates the actual brazing process, which uses the flame temperature to melt the filler and take off after that and let the capillary phenomena works free. The flame heat source is applied by selecting the outer surface of the copper tube thickness in its contact end with the stainless-steel inner tube in ANSYS and using the temperature to it as shown in Figure 15(A); penetration of molten filler across the brazed joint will depend on the wetting process and contact angle between molten filler and base metal. The fluidity and density of molten filler are strongly influenced by temperature, as are the flux and joint overlap surface. When it comes to liquid-solid wetting, a liquid's surface tension (g) and density (r) are critical thermodynamic properties. The diffusion of molten filler into base metals during brazing depends on wetting phenomena and the contact angle value, which is determined by the molten filler's surface tension. According to thermodynamics, surface tension is the energy ratio required to move molecules from a liquid's bulk to its surface, increasing the liquid's surface

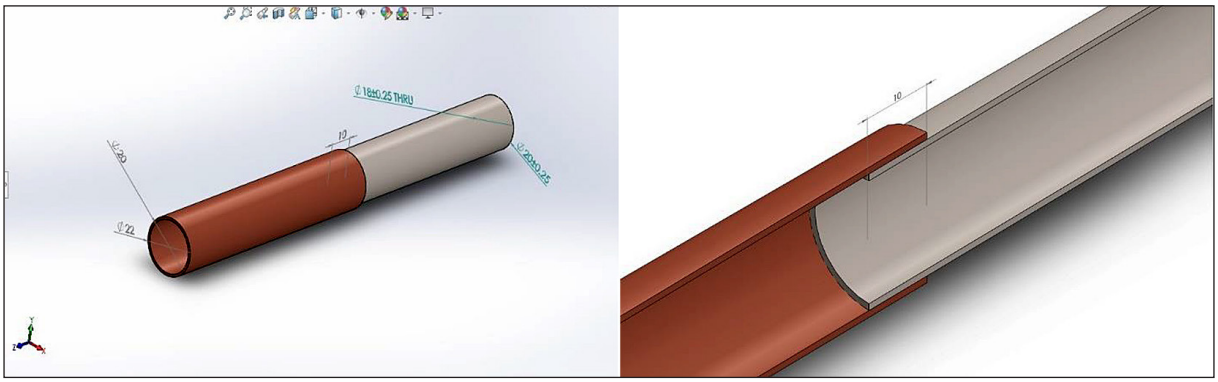

Fig. 13. Solid work geometrical for stainless steel and copper tubes

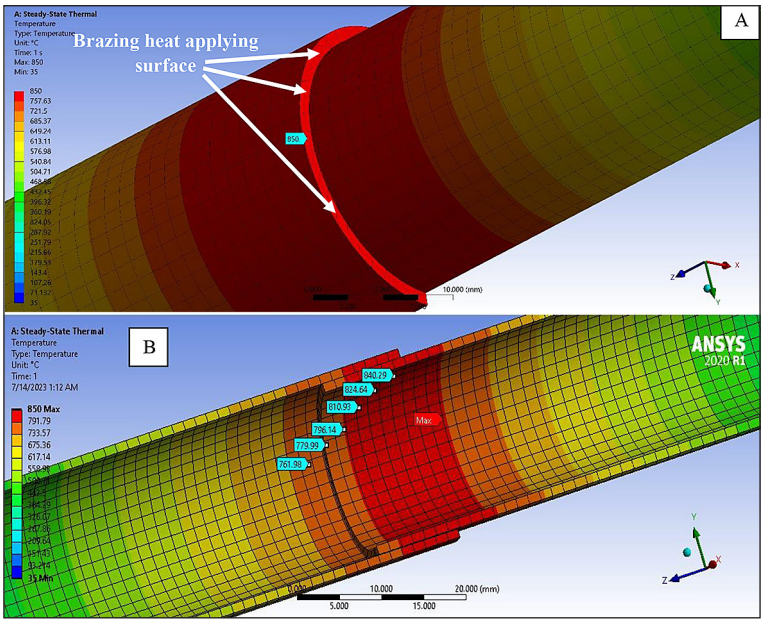

Fig. 15. Heat distribution ANSYS model of (A) Brazing heat applying surface (B) brazing seam with heat prop locations

area [33]. According to the following equation, the density is temperature-dependent, per thermodynamic laws [34]. Suppose we know that C and D are temperature-dependent. C and D are constants used to harmonize the equation. When attempting to ascertain the precise values of these constants for a specific system, it is customary and widely accepted to conduct a meticulous array of experiments to measure the surface tension (γ) and density (ρ) under diverse and varying conditions. In that case, it is apparent from this equation that surface tension is directly proportional to brazing temperature increase, while density is inversely proportional to it.

$$\frac{\gamma}{\rho^2} = C\rho^2 + D \tag{1}$$

Gamma is the molten filler surface tension, ρ is the density, and C and D are parameters depending on temperatures.

The thermal analysis model of brazing heat distribution across the brazed joint illustrated the maximum heat generated at the intersection line between the two tubes or the overlap line. This line is where the brazing filler will be applied to the joint, and the brazing torch will be used to melt the brazing filler and heat the rest of the joint to proceed with brazing by employing the capillary action phenomena. The thermal analysis shows that all the overlap length has thermal gradient inside the melting temperature range of brazing filler, which means molten filler will reach and penetrate until the end of the joint, but due to the temperature drop when moving away from the heat source, density, and surface tension will change. According to that contact angle between molten filler and solid base, the surface will be increased and badly affect the wetting process between molten filler and solid base surface; this analysis is proved by the microstructure image in Figure 7(C), which demonstrates the formation of surface micro-crack at the end of the joint due to lack in adhesion between molten filler and solid stainless steel surface which resulted in high contact angle and lack in joining between the filler and solid surface, that means lack in joining in the intersection line, and this is where the micro-cracks occurred. The Microhardness profile in Figure 12 is also strongly related to the temperature gradients across the brazed joint. The formation of the different phases gives the hardness or softness effect, depending on the molten filler diffusion into a base metal direction and vice versa. According to the following equation, the distribution of these elements will depend on the heat temperature because (Diffusivity increases exponentially).

$$D = D_o \exp(-\frac{Qd}{RT}) \tag{2}$$

where: D is diffusion coefficient (m²/s);
D_o is pre-exponential (m²/s);
Qd is activation energy (J/mol);

R is constant, and finally;
T is the absolute temperature.

All Eq. 2 parameters can be fixed depending on the base metal or the filler type. The only variable in this equation is the temperature, so if we can determine the temperature from the simulation model in the torch brazing process, it is possible to determine the diffusion coefficient of the elements and predicate the resulting phases and intermetallic compound inside the brazing seam. The thermal simulation results in Figures 15(A) and 15(B) showed that the maximum heating temperature recorded in the brazing seam would also result in a very high cooling rate and complex phase formation. The high hardness profile of the brazing seam can certify this. Also, the failure location during the tensile test in the brazing seam for all the tested specimens reflects a good agreement with this analysis. The heat distribution of numerical simulation model results illustrated an excellent deal with experiment results. The understanding of simulation results with experiment results confirmed the validity of the heat distribution model. The torch brazing process depends on the capillary action in its techniques. This phenomenon could move liquid horizontally over long distances. Still, the height or depth that liquid can reach in tiny space between two surfaces is limited by the amount of this space, weight, and the liquid physical properties like the density and the surface tension, which are also related to the temperature, from the capillary phenomena equation in Eq. 3 it is evident that height is directly proportional to surface tension (γ).

In addition, it's worth noting that the height or penetration depth is directly proportional to the distance between two surfaces. A smaller distance (r) increases the molten filler since less space can hold less mass. The fluid density (ρ) is inversely proportional to the liquid height, meaning that a higher density corresponds to a larger mass in the same volume. It can be shown that this height (h) is given by:

$$H = 2\gamma cos\theta/\rho gr \quad (3)$$

From this equation, a strong connection between the molten filler penetration, which is connected to the capillary action phenomena, and the brazing temperature can easily be observed.

The utilization of ANSYS and SOLIDWORKS software to simulate heat distribution is of great significance in the present research paper, as it allows for the comprehensive analysis of various crucial aspects of the brazing process. These aspects include but are not limited to the depth of penetration, the quality of joints, the occurrence of surface cracks, and the wetting process. By this simulation, a profound comprehension of the behavior exhibited by the molten filler material and its interaction with the base metals can be attained, thereby providing invaluable insights that contribute to the optimization of the brazing process. The effectiveness of different brazing techniques and filler materials can be effectively evaluated by analyzing the heat distribution simulation results, thereby guaranteeing the generation of robust joints that possess satisfactory mechanical properties. Furthermore, the outcomes of the simulation can guide the design and optimization of the brazing process, thus facilitating the fabrication of joints devoid of any defects, consequently enhancing the overall quality and reliability of the components subjected to the brazing procedure. Moreover, it is noteworthy that the simulation also plays a pivotal role in the visualization of the heat flow, thereby enabling the identification of any potential issues, such as the presence of surface cracks, which, once detected, can be effectively addressed to augment the overall integrity of the joints. In conclusion, the simulation holds a paramount position in understanding and enhancing the brazing process, thus rendering it an indispensable facet of the research that is presented within the confines of the current paper.

CONCLUSIONS

The present research investigates the evolution of brazed joint microstructure, mechanical properties, and heat distribution along the brazing zone between copper and stainless steel tube joints brazed by torch brazing techniques. According to this study, mechanical test results and the heat distribution ANSYS mathematical model analyses interesting results are found, and the following conclusions can be noticed:

1. The results and analysis of this experiment revealed that the brazed joint mechanical properties of new flux-coated low silver brazing fillers type meet most of the required design criteria of these essential metals hypo structures in many industrial applications, which will further reduce industrial cost.

2. Formation of a ferrite barrier layer between the molten filler metal and stainless steel side is essential to produce a good bonding joint without copper intergranular penetration into the stainless steel grain boundary.
3. Wettability of brazing filler metal on substrate increases with temperature increasing. Wettability will decrease after 780 °C, which results in a lack of bonding and surface crack formation, as provided at the end of the brazed joint when the temperature drops under this level.
4. The maximum wetting area between two kinds of metals and molten filler was achieved at the start of the joint when the temperature was above the filler metal melting temperature, as shown from the SEM images of this zone. In this investigation, the brazing heat thermal distribution.
5. Good agreements between experimental results and the ANSYS heat distribution model give evidence of the effectiveness of this model in studying the maximum and minimum brazing heat location and depth of molten filler penetration inside joint overlap and the effects of the heat distribution on the molten filler density, surface tension, and the capillary action.
6. An excellent metallurgical bonding with both substrates can be produced without microcracks and slag inclusion as soon as the temperature exceeds the filler's melting point.

REFERENCES

1. Fukikoshi T., Watanabe Y., Miyazawa Y., Kanasaki F. Brazing of copper to stainless steel with a low-silver-content brazing filler metal. In: IOP Conference Series: Materials Science and Engineering, 2014; 61(1): 012016.
2. Abdulameer A.G., Mohammed M.S., Abbas A.S. Microstructure variation effects influence on characteristics and mechanical properties of monel 400 and low alloy steel (Astm 387-Gr. 11) Gtaw dissimilar joint. Eastern-European Journal of Enterprise Technologies. 2022; 119(12). https://doi.org/10.15587/1729-4061.2022.266264.
3. Choudhary R.K., Laik A., Mishra P. Microstructure evolution during stainless steel-copper vacuum brazing with a Ag/Cu/Pd filler alloy: effect of nickel plating. Journal of Materials Engineering and Performance. 2017; 26: 1085-1100. https://doi.org/10.1007/s11665-017-2553-6.
4. Jafari M,. Abbasi M., Poursina D., Gheysarian A., Bagheri B. Microstructures and mechanical properties of friction stir welded dissimilar steel-copper joints. Journal of Mechanical Science And Technology. 2017; 31: 1135-1142. https://doi.org/10.1007/s12206-016-1217-z.
5. Srikanth S., Saravanan P., Kumar V., Saravanan D., Sivakumar L., Sisodia S., Ravi K., Jha B. Property Enhancement in metastable 301LN austenitic stainless steel through strain-induced martensitic transformation and its reversion (SIMTR) for metro coach manufacture. Int. J. Metall. Eng. 2013; 2(2): 203-213.
6. Mohamed M.S., Abtan A.A., Moosa A.U. Microstructure and mechanical properties assessments of 304 austenitic stainless steel and monel 400 Dissimilar GTAW Weldment. Journal of Composite & Advanced Materials/Revue des Composites et des Matériaux Avancés. 2023; 33(3). https://doi.org/10.18280/rcma.330301.
7. Ramkumar K.D., Arivazhagan N., Narayanan S. Effect of filler materials on the performance of gas tungsten arc welded AISI 304 and Monel 400. Materials & Design. 2012; 40: 70-79.
8. Shiri S.G., Nazarzadeh M., Sharifitabar M., Afarani M.S. Gas tungsten arc welding of CP-copper to 304 stainless steel using different filler materials. Transactions of Nonferrous Metals Society of China. 2012, 22(12), 2937-2942.
9. Durgutlu A., Gülenç B., Findik F. Examination of copper/stainless steel joints formed by explosive welding. Materials & Design. 2005; 26(6): 497-507.
10. Magnabosco I., Ferro .P, Bonollo F., Arnberg L. An investigation of fusion zone microstructures in electron beam welding of copper-stainless steel. Materials Science and Engineering: A. 2006; 424(1-2): 163-173.
11. Velu M., Bhat S. Metallurgical and mechanical examinations of steel–copper joints arc welded using bronze and nickel-base superalloy filler materials. Materials & Design. 2013; 47: 793-809.
12. Yao C., Xu B., Zhang X., Huang J., Fu J., Wu Y. Interface microstructure and mechanical properties of laser welding copper–steel dissimilar joint. Optics and Lasers in Engineering. 2009, 47(7-8): 807-814.
13. Nowacki J., Danielewski M., Filipek R. Evaluation and computer modelling of mass transport in multicomponent systems in the Au–Ni solder-14-5 PH joints. Journal of Materials Processing Technology. 2004; 157: 213-220.
14. Wang D., Huang J., Tan C., Ma W., Zou Y., Yang Y. Mechanical and corrosion properties of additively manufactured SiC-reinforced stainless steel. Materials Science and Engineering: A. 2022; 841: 143018.
15. Alshalal I., Asaad L.M., Zubaidi F.N. The impact of gas pressure and current on the hardness behaviour of Tig welding stainless steel. In: AIP Conference Proceedings 2022, 2415(1). https://doi.org/10.1063/5.0092615.

16. Fukikoshi T., Watanabe Y., Miyazawa Y., Kanasaki F. Brazing of copper to stainless steel with a low-silver-content brazing filler metal. In: IOP Conference Series: Materials Science and Engineering 2014; 61(1): 012016.
17. Uhlig T., Fedorov V., Elßner M., Wagner G., Weis S. Reduction of liquid metal embrittlement in copper-brazed stainless steel joints. In: IOP Conference Series: Materials Science and Engineering 2017; 181(1): 012032..
18. Nakano J., Malakhov D.V., Purdy G.R. A crystallographically consistent optimization of the Zn–Fe system. Calphad. 2005; 29(4): 276-288.
19. Van Loo F.J. Multiphase diffusion in binary and ternary solid-state systems. Progress in Solid State Chemistry. 1990; 20(1): 47-99.
20. Zhu L., Chen Z., Zhong W.E., Wei C., Cai G., Jiang L., Jin Z., Zhao J.C. Measurement of diffusion coefficients in the bcc phase of the Ti-Sn and Zr-Sn binary systems. Metallurgical and Materials Transactions A. 2019; 50: 1409-1420.
21. Shibli S.M., Meena B.N., Remya R. A review on recent approaches in the field of hot dip zinc galvanizing process. Surface and Coatings Technology. 2015; 262: 210-215.
22. Smith C.S. Grains, phases, and interfaces: An introduction of microstructure. Trans. Metall. Soc. AIME. 1948; 175: 15-51.
23. Chen Y., Yun D., Sui F., Long W., Zhang G., Liu S. Influence of sulphur on the microstructure and properties of Ag–Cu–Zn brazing filler metal. Materials Science and Technology. 2013; 29(10): 1267-1271.
24. Dimitrijević S.P., Manasijević D., Kamberović Ž., Dimitrijević S.B., Mitrić M., Gorgievski M., Mladenović S. Experimental investigation of microstructure and phase transitions in Ag-Cu-Zn brazing alloys. Journal of Materials Engineering and Performance. 2018; 27: 1570-1579.
25. Bobruk E.V., Sauvage X., Zakirov A.M., Enikeev N.A. Tuning the structure and the mechanical properties of ultrafine grain Al–Zn alloys by short time annealing. Reviews on Advanced Materials Science. 2018; 55(1): 61-68.
26. Xue P., Zou Y., He P., Pei Y., Sun H., Ma C., Luo J. Development of low silver AgCuZnSn filler metal for Cu/steel dissimilar metal joining. Metals. 2019; 9(2): 198.
27. Geng Y., Zhang Y., Song K., Jia Y., Li X., Stock H.R., Zhou H., Tian B., Liu Y., Volinsky A.A., Zhang X. Effect of Ce addition on microstructure evolution and precipitation in Cu-Co-Si-Ti alloy during hot deformation. Journal of Alloys and Compounds. 2020; 842: 155666.
28. Khorunov V.F., Stefaniv B.V., Maksymova S.V. Effect of nickel and manganese on structure of Ag–Cu–Zn–Sn system alloys and strength of s. Paton Weld. J. 2014; 4: 22-5.
29. Feng J., Liang S., Guo X., Zhang Y., Song K. Electrical conductivity anisotropy of copper matrix composites reinforced with SiC whiskers. Nanotechnology Reviews. 2019; 8(1): 285-292.
30. Zhang X.H., Zhang Y., Tian B.H., Song K.X., Liu P., Jia Y.L., Chen X.H., An J.C., Zhao Z., Liu Y., Volinsky A.A. Review of nano-phase effects in high strength and conductivity copper alloys/ Nanotechnol. Rev. 2019; 8(1): 383-395.
31. Gangadharan S., Sivakumar D., Venkateswaran T., Kulkarni K. Evolution of microstructure in s of austenitic-martensitic stainless steel with pure silver obtained with Ag-27Cu-5Sn Brazing filler material. Metallurgical and Materials Transactions A. 2016; 47: 6148-6159. doi: 10.1007/s11661-016-3787-x.
32. Kozlova O., Braccini M., Voytovych R., Eustathopoulos N., Martinetti P., Devismes M.F. Brazing copper to alumina using reactive CuAgTi alloys. Acta Materialia. 2010; 58(4): 1252-1260.
33. Yang Y.Y., Zhu Y.M., Peng J.L., Chen J.C., Feng P.P., Huang Z.Q. Excess thermodynamic functions derived from densities and surface tensions of (p-or o-xylene+ ethylene glycol dimethyl ether) between the temperatures (298.15 and 308.15) K. The Journal of Chemical Thermodynamics. 2009; 41(9): 1000-1006.
34. Parsafar G., Kermanpour F., Najafi B. Prediction of the temperature and density dependencies of the parameters of the average effective pair potential using only the LIR equation of state. The Journal of Physical Chemistry B. 1999; 103(34): 7287-92.